Atmos. Chem. Phys. Discuss., 13, 31607–31634, 2013
www.atmos-chem-phys-discuss.net/13/31607/2013/
doi:10.5194/acpd-13-31607-2013

Atmospheric Chemistry and Physics Discussions
Open Access

Technical Note: SWIFT – a fast semi-empirical model for polar stratospheric ozone loss

M. Rex[1], S. Kremser[2], P. Huck[2], G. Bodeker[2], I. Wohltmann[1], M. L. Santee[3], and P. Bernath[4]

[1]Alfred Wegener Institute for Polar and Marine Research, Potsdam, Germany
[2]Bodeker Scientific, Alexandra, New Zealand
[3]Jet Propulsion Laboratory, California Institute of Technology, Pasadena, California, USA
[4]Old Dominion University, Norfolk, VA, USA

Received: 16 October 2013 – Accepted: 13 November 2013 – Published: 2 December 2013

Correspondence to: M. Rex (markus.rex@awi.de)

Published by Copernicus Publications on behalf of the European Geosciences Union.

Abstract

An extremely fast model to estimate the degree of stratospheric ozone depletion during polar winters is described. It is based on a set of coupled differential equations that simulate the seasonal evolution of vortex-averaged hydrogen chloride (HCl), nitric acid (HNO_3), chlorine nitrate ($ClONO_2$), active forms of chlorine ($ClO_x = Cl+ClO+2ClOOCl$) and ozone (O_3) on isentropic levels within the polar vortices. Terms in these equations account for the chemical and physical processes driving the time rate of change of these species. Eight empirical fit coefficients associated with these terms are derived by iteratively fitting the equations to vortex-averaged satellite-based measurements of HCl, HNO_3 and $ClONO_2$ and observationally derived ozone loss rates. The system of differential equations is not stiff and can be solved with a time step of one day, allowing many years to be processed per second on a standard PC. The inputs required are the daily fractions of the vortex area covered by polar stratospheric clouds and the fractions of the vortex area exposed to sunlight. The resultant model, SWIFT (Semi-empirical Weighted Iterative Fit Technique), provides a fast yet accurate method to simulate ozone loss rates in polar regions. SWIFT's capabilities are demonstrated by comparing measured and modeled total ozone loss outside of the training period.

1 Introduction

The importance of stratospheric ozone as a climate active gas has long been recognized (e.g. Forster and Shine, 1997; Gauss et al., 2006; Forster et al., 2007). Accounting for the interactions between climate change and ozone in climate models is usually accomplished by interactively coupling a stratospheric chemistry module to a global climate model (GCM): dynamical fields from the GCM provide input to the stratospheric chemistry module at a time step compatible with the GCM. The ozone fields generated by the chemistry module are returned to the GCM, which uses them to calculate the radiative forcing. The radiative forcing induces changes in atmospheric temperatures which in turn influence dynamics, the distribution of

ACPD
13, 31607–31634, 2013

trace gases and temperature-dependent chemistry. Such models, generally referred to as chemistry-climate models (Austin, 2002; Eyring et al., 2006, 2007), are very computationally expensive. Thus, applying them to multiple greenhouse gas (GHG) or ozone depleting substance (ODS) emissions scenarios is prohibitive. The effects of ozone on climate are therefore usually incorporated into GCMs by prescribing ozone as an external boundary condition. However, this approach results in modeled ozone fields that are not internally consistent with the future evolution of the atmosphere in the GCM. Furthermore, prescribed ozone fields are unlikely to be aligned with the internal dynamics of the model, i.e. values typical of the polar vortex may be specified in regions outside of the vortex as a result of vortex excursions within the model, or lower stratospheric air may be prescribed in the upper troposphere if the model has an anomalously high tropopause on that day. In such a model configuration atmospheric dynamics cannot interact with polar ozone chemistry. Incoherence between prescribed ozone and the GCM dynamics is likely to affect ozone radiative forcing and the resultant pattern of surface climate change. Thus, there is an urgent need for fast stratospheric chemistry schemes that can be incorporated into GCMs.

A number of fast stratospheric chemistry schemes have been developed. The Cariolle scheme (Cariolle and Déqué, 1986) expands the ozone continuity equation as a Taylor series up to first order around three variables, that is, the local value of the ozone mixing ratio, the temperature, and the overhead ozone column. The 8 coefficients for the resultant terms in the expansion are derived from a 2-D photochemical model, independently for each latitude and altitude. The scheme has been used in GCMs to model ozone-climate interactions (Braesicke et al., 2006) and in chemical transport models to simulate ozone trends (Hadjinicolaou et al., 2005).

Linoz (McLinden et al., 2000; Hsu and Prather, 2009) is similar to the Cariolle scheme and calculates the net production of ozone as a function of the same three variables as the Cariolle scheme. Small perturbations about a chemical climatology are used to calculate coefficients of a Taylor series expansion of the net production in terms of these three variables. The system is highly constrained, with 7 tables

ACPD
13, 31607–31634, 2013

each providing 216 profiles of parameters. Version 1 of Linoz excluded heterogeneous chemistry, and as a result there was no Antarctic ozone hole and no enhanced Arctic ozone loss during cold winters. Version 2 incorporates the polar stratospheric cloud (PSC) parameterization scheme of Cariolle et al. (1990). Both the Cariolle and Linoz schemes rely on a statistical representation of the sensitivity of the ozone tendency to the three controlling variables and are therefore unlikely to be applicable outside of the dataset on which they were trained. The FASTOC scheme (Bourqui et al., 2005) uses a large set of pre-computed transfer functions to mimic the response of a stratospheric chemical box model. It is not tuned to present-day conditions and does not include any relaxation to a prescribed climatology in the region of active chemistry.

The SWIFT (Semi-empirical Weighted Iterative Fit Technique) model described in this paper is entirely different from the Cariolle and Linoz schemes. It is a semi-empirical model as defined in the approach of Huck et al. (2013). The first version of SWIFT described in this paper includes heterogeneous polar ozone depletion only, which is by far the strongest anthropogenic perturbation of the state of the ozone layer. A version that includes full treatment of extra-polar processes is in development. Rather than linearizing perturbations about some climatological state, it describes the seasonal evolution of the key trace gases driving ozone destruction in a set of coupled first order differential equations. The equations have terms based on the chemical and physical processes known to affect the time evolution of these species. The model is not required to be linear and can cope well with the significant non-linearities occurring in polar ozone chemistry. The model is described in detail in Sect. 2, and a demonstration of its capabilities is presented in Sect. 3.

2 Model description

The purpose of SWIFT is to provide a simple, easy to use and numerically efficient process-based description of polar ozone loss. The focus is on numerical efficiency while maintaining the physical and chemical properties of the polar ozone loss process.

ACPD
13, 31607–31634, 2013

The model is applicable under a wide range of meteorological and climatic conditions, including future conditions.

To include the chemical mechanisms that are relevant for polar ozone loss the model describes the evolution of four prognostic variables ($ClONO_2$, HCl, total HNO_3, and O_3) and two diagnostic variables (ClO_x and HNO_3 in the gas phase) throughout winter, starting from prescribed initial conditions. All variables are vortex averages of the respective species. A system of coupled differential equations describes the changes of the prognostic variables due to the relevant chemical mechanisms. The diagnostic variables are derived from the prognostic variables at each time step. The model is driven by the daily values of the fractional vortex area that is cold enough to allow the existence of PSCs (Fractional Area of PSCs, FAP) and by the 24 h average of the fraction of the vortex area that is exposed to sunlight (Fractional Area of Sunlight, FAS). Time series of FAP and FAS throughout the winter are derived from ECMWF (European Centre for Medium Range Weather Forecasts) ERA Interim meteorological reanalyses (Dee et al., 2011).

SWIFT is a model of chemical processes that influence polar ozone. It does not explicitly include transport-related changes in ozone, but these changes are implicitly included in the fit parameters, which are fitted on time series of satellite data. Hence, the model should not be used in combination with a model of stratospheric transport in the current version. In this initial version of SWIFT, the model runs are performed on one fixed potential temperature surface close to the altitude where maximum ozone loss occurs. This approach neglects the influence of vertical transport (i.e. slow diabatic subsidence) on the time evolution of the prognostic variables. For ClO_x, $ClONO_2$, HCl and HNO_3 the chemically induced rates of change are much larger than the slow changes due to cross-isentropic transport, and the excellent performance of the model (see Sect. 3) justifies this approach. But for ozone, particularly in the Arctic, the rate of change from diabatic subsidence is on the same order of magnitude as the chemically induced ozone change. Therefore, in its current version, SWIFT should only be used to calculate ozone loss rates rather than the absolute abundance of ozone. In the future,

ACPD
13, 31607–31634, 2013

SWIFT will include a transport module to allow for mixing across the vortex edge and for the effect of subsidence within the vortex.

2.1 Model equations

Polar ozone chemistry is well understood (e.g. review articles by Solomon, 1999, or von Hobe et al., 2013). Rather than encapsulating this chemistry in full detail, the SWIFT model is conceptual, i.e. instead of representing each individual chemical reaction by individual terms in the equations (as is done in full chemical transport models), the bulk effect of chemical mechanisms is considered.

More than 90 % of the overall chemical loss of ozone during polar winter is due to the combined effect of the ClO + ClO, ClO + BrO and ClO + O catalytic ozone destruction cycles (Frieler et al., 2006). Figure 1a shows that the 24 h average ozone loss rate by these cycles is a fairly linear function of the concentration of ClO_x (Cl + ClO + 2 ClOOCl). The reason is that non-linearities in the dominating ClO + ClO and ClO + BrO cycles mostly cancel (Fig. 1b and c).

Since ozone loss can only occur in sunlight, it is also a function of the time that the air mass is exposed to sunlight. Hence, the vortex-average ozone loss can be written as:

$$\frac{dO_3}{dt} = -D \tag{1}$$

with

$$D = d \cdot [ClO_x] \cdot FAS \tag{2}$$

where [...] denotes the mixing ratio of a species and d is an empirically determined fit parameter (as the parameters a–h and z in the following equations). The detailed approach to determine the values of the parameters is described in Sect. 2.3. In principle d can also be derived from Fig. 1, which would link d to the kinetic parameters in the model that has been used to produce Fig. 1.

ACPD
13, 31607–31634, 2013

Equation (2) shows that estimating the vortex-average ozone loss rate requires good estimates of the evolution of ClO_x through the winter. To estimate ClO_x, the model needs to represent the key mechanisms that convert the reservoir species $ClONO_2$ and HCl into ClO_x and vice versa. Once the concentrations of $ClONO_2$ and HCl have been determined, the concentration of ClO_x is calculated from:

$$[ClO_x] = [Cl_y] - [HCl] - [ClONO_2] \tag{3}$$

where $[Cl_y]$ is the overall amount of inorganic chlorine, which can be assumed to be constant in an individual air mass during any given polar winter.

The evolution of vortex-averaged $ClONO_2$ and HCl is estimated by:

$$\frac{d[ClONO_2]}{dt} = B - A - G - H \tag{4}$$

and

$$\frac{d[HCl]}{dt} = C + F - A \tag{5}$$

where A, B, C, F, G and H represent the effects of chlorine activation and deactivation by the chemical mechanisms described in Sects. 2.1.1 and 2.1.2.

The model equations are summarized in Table 1 and the terms used in the equations are given in Table 2. These terms are described in detail below.

2.1.1 Chlorine activation mechanisms

Term A describes the loss of $ClONO_2$ and HCl and the production of ClO_x due to the heterogeneous reaction

$$HCl + ClONO_2 \rightarrow Cl_2 + HNO_3 \tag{R1}$$

followed by the photolysis of Cl_2

$$Cl_2 + h\nu \rightarrow 2\,Cl \tag{R2}$$

ACPD
13, 31607–31634, 2013

Cl_2 photolyses readily at wavelengths longer than those required for the ozone loss process. Hence, at sunrise most Cl_2 that may have formed during night will photolyse before the sun is high enough for efficient ozone loss to occur. During day Cl_2 cannot build up in significant quantities. Therefore, the photolysis step can be ignored in a conceptual model of the ozone loss process. In terms of ozone loss the system of Reactions (R1) and (R2) is equivalent to a system that directly produces ClO_x in the initial heterogeneous Reaction (R1). Unless HCl is very low, the rate of Reaction (R1) depends only on the surface area density of the PSC particles and the concentration of $ClONO_2$:

$$A = a \cdot [ClONO_2] \cdot [HNO_3] \cdot FAP \tag{6}$$

The factor $[HNO_3] \cdot FAP$ represents the availability of reactive surfaces in a vortex-average bulk sense.

Only when HCl concentrations become very low is the reaction also limited by the uptake rate of HCl on the PSC particles. The rate of Reaction (R1) then also depends on HCl concentrations. For HCl concentrations below 1 % of Cl_y, A is defined as:

$$A = a \cdot [HCl] \cdot [ClONO_2] \cdot [HNO_3] \cdot FAP \tag{7}$$

Term G represents the effect of

$$ClONO_2 + h\nu \rightarrow Cl + NO_3 \tag{R3}$$

The efficiency of this process depends on the concentration of $ClONO_2$ and the availability of sunlight:

$$G = g \cdot [ClONO_2] \cdot FAS \tag{8}$$

During winter this is a minor loss channel for $ClONO_2$, but in spring it controls the repartitioning between $ClONO_2$ and HCl in the Arctic. With the exception of the last few

ACPD
13, 31607–31634, 2013

weeks in Arctic winters, the model would do well without this term, and it is not very important for the calculated ozone loss.

Term H accounts for the effect of the heterogeneous reaction

$$ClONO_2 + H_2O \rightarrow HOCl + HNO_3 \quad \text{(R4)}$$

followed by photolysis of HOCl

$$HOCl + h\nu \rightarrow Cl + OH \quad \text{(R5)}$$

Reaction (R5) is rapid during daytime. For the purpose of the conceptual model it can be included in Reaction (R4) based on the same arguments that have been discussed for the Cl_2 photolysis in term A. Reaction (R4) is efficient only at temperatures well below the PSC formation temperature threshold. If FAP is large, temperatures in the core part of the cold region will typically be well below the PSC formation temperature threshold so that term H starts to become relevant. Hence this mechanism is assumed to start being efficient only if FAP exceeds a certain threshold, which is represented by the parameter y:

$$H = h \cdot [ClONO_2] \cdot \max((FAP - y), 0) \quad (9)$$

Equation (9) uses only the fraction of FAP that exceeds the threshold of y, assuming that only in the central region of large PSC areas temperatures will be sufficiently low to make Reaction (R4) efficient.

2.1.2 Chlorine deactivation mechanisms

Term B describes the chlorine deactivation by formation of $ClONO_2$, which results from the photolysis of HNO_3 followed by the fast reaction of NO_2 with ClO:

$$HNO_3 + h\nu \rightarrow NO_2 + OH \quad \text{(R6)}$$

$$NO_2 + ClO + M \rightarrow ClONO_2 + M \quad \text{(R7)}$$

ACPD
13, 31607–31634, 2013

Unless ClO concentrations are very low, Reaction (R7) is fast and can be ignored in the conceptual model:

$$B = b \cdot [HNO_3]_g \cdot FAS \tag{10}$$

i.e. $ClONO_2$ is assumed to directly form from Reaction (R6). $[HNO_3]_g$ denotes the mixing ratio of HNO_3 in the gas phase.

If ClO_x, and hence ClO, are very low, Reaction (R7) also limits the production of $ClONO_2$. For ClO_x less than 5 % of Cl_y

$$B = b \cdot [ClO_x] \cdot [HNO_3]_g \cdot FAS \tag{11}$$

is used.

Term C represents the effect of

$$Cl + CH_4 \rightarrow HCl + CH_3 \tag{R8}$$

This reaction is responsible for deactivation under ozone hole conditions. Once ozone concentrations become very low, the reaction

$$Cl + O_3 \rightarrow ClO + O_2 \tag{R9}$$

becomes less efficient and the ratio of Cl over ClO increases with $1/[O_3]$. Since ClO_x is mainly in the form of ClOOCl during nighttime, Reaction (R8) can only occur during daytime. Hence its efficiency depends on $[ClO_x]$, FAS and $1/[O_3]$:

$$C = c \cdot [ClO_x] \cdot FAS/[O_3] \tag{12}$$

Term F represents the net effect of the ≈ 8 % channel of the reaction of ClO with OH, which results in HCl formation:

$$ClO + OH \rightarrow HCl + O_2 \tag{R10}$$

ACPD
13, 31607–31634, 2013

This reaction helps HCl reformation in both hemispheres, but only in late winter since both $[ClO]/[ClO_x]$ and OH scale with the availability of sunlight. The effect of Reaction (R10) is described by

$$F = f \cdot [ClO_x] \cdot FAS^2 \tag{13}$$

Since significant dehydration occurs in the Antarctic, the late winter abundance of total water is reduced to about 25 % of the levels commonly found in the Arctic, also reducing the concentrations of OH by the same factor. Therefore an additional scaling factor of 0.25 is used in the term F for the Antarctic:

$$F = 0.25f \cdot [ClO_x] \cdot FAS^2 \tag{14}$$

2.1.3 Sequestration and irreversible removal of HNO_3

The processes described above regulate the balance between ClO_x and the reservoir gases HCl + $ClONO_2$. Other than FAP and FAS, the only remaining inputs required to solve the model equations are total and gas-phase HNO_3 (c.f. Terms A and B in Sects. 2.1.1 and 2.1.2).

Because of strong denoxification during polar winter (heterogeneous conversion of NO_x into HNO_3 on cold background aerosol, where NO_x denotes the sum of all short-lived nitrogen oxides), N_2O, HNO_3 and $ClONO_2$ are the only nitrogen oxide species that exist at significant abundances at that time. Under polar winter conditions N_2O is inert, and the abundance of $ClONO_2$ is about an order of magnitude smaller than that of HNO_3. Hence, the total abundance of HNO_3 is not altered much by chemistry during polar winter.

The only process that significantly changes total HNO_3 in the model is denitrification, i.e. the irreversible removal of HNO_3 due to sedimentation of HNO_3-containing particles. Denitrification only occurs if either individual PSC particles persist sufficiently long (many days) to grow to sizes of a few micrometers, or if temperatures fall so low that water ice can accumulate on the PSC particles, which lets them grow rapidly.

ACPD
13, 31607–31634, 2013

Both processes require large values of FAP: the slow growth of particles can only occur if air mass trajectories exist that stay within the potential PSC region for many days, requiring large PSC areas. Furthermore, when ice temperatures are reached, conditions are very cold and PSC areas are typically very large. Hence, in the model, the denitrification process is only triggered if the threshold value y for FAP is exceeded:

$$\frac{\mathrm{d}[\mathrm{HNO_3}]}{\mathrm{d}t} = -E \tag{15}$$

with

$$E = e \cdot [\mathrm{HNO_3}] \cdot \max((\mathrm{FAP} - y), 0) \tag{16}$$

The fraction of HNO_3 in the gas phase is calculated from the total HNO_3 abundance at each time step by:

$$[\mathrm{HNO_3}]_\mathrm{g} = [\mathrm{HNO_3}] \cdot (1 - \mathrm{FAP}) + z \cdot [\mathrm{HNO_3}] \cdot \mathrm{FAP} \tag{17}$$

The first term represents the gas-phase HNO_3 outside of the area where temperatures are below the PSC formation threshold (here gas phase equals total), and the second term includes the average fraction z of HNO_3 still in the gas phase in areas where temperatures are below the PSC threshold. The latter includes the fact that PSCs will only form in parts of the region where they are thermodynamically stable, due to the nucleation barrier (Pitts et al., 2007).

2.2 Initialization

The prognostic variables are initialized at the beginning of the winter (1 December in the Arctic and 20 May in the Antarctic). Since the model is conceptual at this stage, the abundances of the chemical species are normalized, and the initial concentrations for

ACPD
13, 31607–31634, 2013

the three different families are set to unity:

$$[O_3](t = 0) = 1 \quad (18)$$

$$[HNO_3](t = 0) = 1 \quad (19)$$

$$[Cl_y](t = 0) = 1 \quad (20)$$

The partitioning of Cl_y between HCl and $ClONO_2$ is taken from Fig. 1 of Harris et al. (2010), which is based on an analysis by Santee et al. (2008) of data from the Microwave Limb Sounder (MLS, Livesey et al., 2011) on the Aura satellite and data from the Fourier Transform Spectrometer, which is part of the Atmospheric Chemistry Experiment (ACE-FTS, Bernath et al., 2005):

$$[HCl](t = 0) = 0.65[Cl_y] \quad (21)$$

$$[ClONO_2](t = 0) = 0.35[Cl_y] \quad (22)$$

For long-term studies, the secular variation of $[Cl_y]$ can also be set to represent the long-term evolution of Equivalent Effective Stratospheric Chlorine (EESC; e.g. Newman et al., 2007), an estimate of the total effective amount of halogens in the stratosphere. To compare the normalized model abundances with observations of vortex-averaged mixing ratios, the following scaling factors have been used:

$$F_{Cl_y} = 2.7 \times 10^{-9} \quad (23)$$

$$F_{HNO_3} = 10.6 \times 10^{-9} \quad (24)$$

$$F_{dO_3/dt} = 42.7 \times 10^{-9}\ \mathrm{day}^{-1} \quad (25)$$

These factors were determined by dividing the averaged normalized model results by vortex averaged observations from Match (for $d[O3]/dt$), MLS (for [HCl] and $[HNO_3]$) and ACE-FTS (for $[ClONO_2]$). Match is an approach to derive chemical ozone loss rates from coordinated ozonesonde observations (e.g. Rex et al., 1998). $[Cl_y]$ has been determined from the sum of [HCl] and $[ClONO_2]$ at the beginning of the winter.

ACPD
13, 31607–31634, 2013

A model with initial concentrations based on the scaling factors would give identical results to the normalized formulation described here. It would then calculate absolute values for the vortex-average mixing ratios and ozone loss rates rather than the normalized values shown here. The normalization moves the degrees of freedom, which usually are in the model initialization, to the scaling factors, an approach that is convenient for such a conceptual model.

2.3 Training of the model

The fit coefficients *a*–*h*, *y* and *z* of SWIFT (Table 3) are chosen such that the model best represents measurements of HCl, $ClONO_2$, gas-phase HNO_3 and ozone loss rates as derived from observations. For this procedure, HCl and HNO_3 measurements from MLS, $ClONO_2$ from ACE-FTS and ozone loss rates from Match are used. For HCl, $ClONO_2$ and HNO_3, vortex averages have been calculated from the individual data points, and the vortex averages on the retrieval surfaces have been interpolated to the potential temperature surface of 460 K that is used in the model. Ozone loss rates from Match represent vortex averages and have been retrieved on the model level.

FAP and FAS are calculated by assuming the vortex edge at the 31.2 PVU potential vorticity contour. The area where the formation of nitric acid trihydrate (NAT) polar stratospheric clouds is possible is calculated from the equations given in Hanson and Mauersberger (1988) and divided by the vortex area to give FAP. For FAS, the area above a solar zenith angle of 95° in the vortex is calculated and divided by the vortex area.

The model is trained on the seasonal evolution of these quantities during one Arctic winter (2004/2005) and one Antarctic winter (2006). In the Antarctic, Match ozone loss rates are only available for winter 2003, but MLS and ACE-FTS data is not available for 2003. Since the meteorology during the 2003 Antarctic winter was reasonably similar to that in 2006, and FAP and FAS for these two Antarctic winters are not significantly different, we have used the ozone loss rates from the Match campaign in 2003 for the 2006 Antarctic winter.

ACPD
13, 31607–31634, 2013

The interannual variability of ozone loss is not used to train the model and can be used to validate the ability of the model to reproduce ozone loss under a wide range of meteorological conditions.

To train SWIFT, the model parameters are fitted to minimize a cost function, which is defined as the sum of the absolute values of the differences between all observations (divided by the scale factors) and the corresponding model values. For the ozone loss rates, the individual differences were weighted by the reciprocal of the uncertainty of the respective observation. For HCl and $ClONO_2$, the individual uncertainties of the vortex-averaged observations are assumed to be equal for all dates.

Calculating the differences from the normalized data ensures that the same weights are used for all chemical species, independent of their absolute abundance. But since ozone loss rates are two orders of magnitude smaller than the normalized abundances of the chemical species (ozone loss rates are on the order of % per day), their differences were multiplied by 50 to give them a weight in the cost function that is comparable to that of the chemical species. In addition, the ozone loss rates of the model have been averaged over 14 days to match the time resolution of the Match ozone loss rate observations.

The average differences are calculated individually for all species, and these averages are summed to give the cost function, weighted by the reciprocal of the average uncertainty of the measurements of that species. This results in identical weights for all species even if the number of available measurements is different.

The numerical algorithm described in Huck et al. (2013) has been used to solve the optimization problem. The set of parameters determined by the optimization procedure is listed in Table 3. To limit the degrees of freedom in the fitting procedure, the "PSC threshold" parameter y has not been fitted but is estimated from Fig. 2.13 of WMO (2011).

ACPD
13, 31607–31634, 2013

3 Results

Figures 2 and 3 show the evolution of the model species throughout the Arctic winter 2004/05 and the Antarctic winter 2006, respectively. Overall, the model reproduces the seasonal evolution of the key species and of the observed ozone loss rates throughout these winters well.

To assess the interannual variation of the calculated ozone loss, the time integrated normalized mixing ratio loss at 460 K (i.e. a value ranging from zero for no loss to one for complete loss of ozone) is used as a proxy for the column ozone loss, by multiplying it with a factor of 260 DU. This factor has been determined by fitting the normalized mixing ratios to column loss observations. Figure 4 shows the interannual variation of the proxy total ozone loss compared with total ozone loss observations (updated from Rex et al., 2006). The agreement of the absolute values is caused by fitting the scaling factor to observations, but the correlation between the time series is striking.

4 Discussion and conclusions

In this work, a semi-empirical approach to modeling stratospheric ozone loss in both the Arctic and Antarctic has been developed with the goal of simulating as faithfully as possible the chemical mechanisms that drive polar ozone loss with a simple and fast model of vortex average quantities.

SWIFT provides a good representation of polar ozone loss for a wide range of vortex conditions in the current climate, including the range between warm and disturbed Arctic winters to the coldest Antarctic winters. The mechanisms in SWIFT are chemically and physically representative of real-world processes. SWIFT is extremely fast and processes several hundreds of years per second.

SWIFT includes parameters for the individual chemical mechanisms that replace the reaction kinetic parameters of full chemical models. In principle, most of these parameters can be linked to the underlying reaction kinetic parameters that are usually

ACPD
13, 31607–31634, 2013

determined from laboratory measurements. However, in SWIFT these parameters are trained on observations of the atmosphere, rather than on observations in the laboratory. It is important to note that these empirical parameters are intrinsic physical properties of the involved molecules and mechanisms, and do not change with changing climate conditions. Hence SWIFT will still give a good representation of the chemical conditions inside the polar vortices in a changing climate, unless the meteorological conditions become so drastically different from the range of present-day conditions that currently unimportant mechanisms become relevant. However, climate models do not suggest that such dramatic climate change will occur during the next century or so.

SWIFT includes all major feedbacks between climate change and polar ozone loss. However, in its current version SWIFT does not include all potential feedbacks, e.g., changes in stratospheric age of air or changes of NO_y or total sulfate are currently not accounted for, but many of these can be included in future versions of the model.

The semi-empirical model described here can also be used for the ozone loss in individual air masses as a semi-empirical box model. The parameters FAP and FAS would then be defined to give the fractional time the individual air mass spends in PSC conditions or in sunlight, respectively, and a different set of fitting parameters has to be determined, e.g., by using a box model with full chemistry for the training of the semi-empirical model.

Acknowledgements. This work was supported by the BMBF under the FAST-O3 project in the MiKliP framework programme (FKZ 01LP1137A). Work at Bodeker Scientific was supported in part by a New Zealand Antarctic Research Institute funded project. The ACE mission is supported primarily by the Canadian Space Agency. We thank ECMWF for providing reanalysis data. Work at the Jet Propulsion Laboratory, California Institute of Technology, was done under contract with the National Aeronautics and Space Administration.

ACPD
13, 31607–31634, 2013

References

Austin, J.: A three-dimensional coupled chemistry-climate model simulation of past stratospheric trends, J. Atmos. Sci., 59, 218–232, 2002. 31609

Bernath, P. F., McElroy, C. T., Abrams, M. C., Boone, C. D., Butler, M., Camy-Peyret, C., Carleer, M., Clerbaux, C., Coheur, P.-F., Colin, R., DeCola, P., DeMazière, M., Drummond, J. R., Dufour, D., Evans, W. F. J., Fast, H., Fussen, D., Gilbert, K., Jennings, D. E., Llewellyn, E. J., Lowe, R. P., Mahieu, E., McConnell, J. C., McHugh, M., McLeod, S. D., Michaud, R., Midwinter, C., Nassar, R., Nichitiu, F., Nowlan, C., Rinsland, C. P., Rochon, Y. J., Rowlands, N., Semeniuk, K., Simon, P., Skelton, R., Sloan, J. J., Soucy, M.-A., Strong, K., Tremblay, P., Turnbull, D., Walker, K. A., Walkty, I., Wardle, D. A., Wehrle, V., Zander, R., and Zou, J.: Atmospheric Chemistry Experiment (ACE): mission overview, Geophys. Res. Lett., 32, L15S01, doi:10.1029/2005GL022386, 2005. 31619

Bourqui, M. S., Taylor, C. P., and Shine, K. P.: A new fast stratospheric ozone chemistry scheme in an intermediate general-circulation model, II: application to effects of future increases in greenhouse gases, Q. J. Roy. Meteor. Soc., 131, 2243–2261, 2005. 31610

Braesicke, P., Hurwitz, M. M., and Pyle, J. A.: The stratospheric response to changes in ozone and carbon dioxide as modelled with a GCM including parameterised ozone chemistry, Meteorol. Z., 15, 343–354, 2006. 31609

Cariolle, D. and Déqué, M.: Southern hemisphere medium-scale waves and total ozone disturbances in a spectral general circulation model, J. Geophys. Res., 91, 10825–10846, 1986. 31609

Cariolle, D., Lasserre-Bigory, A., and Royer, J. F.: A general circulation model simulation of the springtime Antarctic ozone and its impact on mid-latitudes, J. Geophys. Res., 95, 1883–1898, 1990. 31610

Dee, D. P., Uppala, S. M., Simmons, A. J., Berrisford, P., Poli, P., Kobayashi, S., Andrae, U., Balmaseda, M. A., Balsamo, G., Bauer, P., Bechtold, P., Beljaars, A. C. M., van de Berg, L., Bidlot, J., Bormann, N., Delsol, C., Dragani, R., Fuentes, M., Geer, A. J., Haimberger, L., Healy, S. B., Hersbach, H., Hólm, E. V., Isaksen, L., Kållberg, P., Köhler, M., Matricardi, M., McNally, A. P., Monge-Sanz, B. M., Morcrette, J.-J., Park, B.-K., Peubey, C., de Rosnay, P., Tavolato, C., Thépaut, J.-N., and Vitart, F.: The ERA-Interim reanalysis: configuration and performance of the data assimilation system, Q. J. Roy. Meteor. Soc., 137, 553–597, 2011. 31611

ACPD
13, 31607–31634, 2013

SWIFT – a fast model for polar stratospheric ozone loss

M. Rex et al.

Eyring, V., Butchart, N., Waugh, D. W., Akiyoshi, H., Austin, J., Bekki, S., Bodeker, G. E., Boville, B. A., Brühl, C., Chipperfield, M. P., Cordero, E., Dameris, M., Deushi, M., Fioletov, V. E., Frith, S. M., Garcia, R. R., Gettelman, A., Giorgetta, M. A., Grewe, V., Jourdain, L., Kinnison, D. E., Mancini, E., Manzini, E., Marchand, M., Marsh, D. R., Nagashima, T., Newman, P. A., Nielsen, J. E., Pawson, S., Pitari, G., Plummer, D. A., Rozanov, E., Schraner, M., Shepherd, T., Shibata, K., Stolarski, R. S., Struthers, H., Tian, W., and Yoshiki, M.: Assessment of temperature, trace species, and ozone in chemistry-climate model simulations of the recent past, J. Geophys. Res., 111, D22308, doi:10.1029/2006JD007327, 2006. 31609

Eyring, V., Waugh, D. W., Bodeker, G. E., Cordero, E., Akiyoshi, H., Austin, J., Beagley, S. R., Boville, B. A., Braesicke, P., Brühl, C., Butchart, N., Chipperfield, M. P., Dameris, M., Deckert, R., Deushi, M., Frith, S. M., Garcia, R. R., Gettelman, A., Giorgetta, M. A., Kinnison, D. E., Mancini, E., Manzini, E., Marsh, D. R., Matthes, S., Nagashima, T., Newman, P. A., Nielsen, J. E., Pawson, S., Pitari, G., Plummer, D. A., Rozanov, E., Schraner, M., Scinocca, J. F., Semeniuk, K., Shepherd, T. G., Shibata, K., Steil, B., Stolarski, R. S., Tian, W., and Yoshiki, M.: Multimodel projections of stratospheric ozone recovery in the 21st century, J. Geophys. Res., 112, D16303, doi:10.1029/2006JD008332, 2007. 31609

Forster, P. M. and Shine, K. P.: Radiative forcing and temperature trends from stratospheric ozone changes, J. Geophys. Res., 102, 10841–10855, 1997. 31608

Forster, P. M., Bodeker, G. E., Schofield, R., Solomon, S., and Thompson, D. W. J.: Effects of ozone cooling in the tropical lower stratosphere and upper troposphere, Geophys. Res. Lett., 34, L23813, doi:10.1029/2007GL031994, 2007. 31608

Frieler, K., Rex, M., Salawitch, R. J., Canty, T., Streibel, M., Stimpfle, R., Pfeilsticker, K., Dorf, M., Weisenstein, D. K., and Godin-Beekman, S.: Towards a better quantitative understanding of polar stratospheric ozone loss, Geophys. Res. Lett., 33, L10812, doi:10.1029/2005GL025466, 2006. 31612

Gauss, M., Myhre, G., Isaksen, I. S. A., Grewe, V., Pitari, G., Wild, O., Collins, W. J., Dentener, F. J., Ellingsen, K., Gohar, L. K., Hauglustaine, D. A., Iachetti, D., Lamarque, F., Mancini, E., Mickley, L. J., Prather, M. J., Pyle, J. A., Sanderson, M. G., Shine, K. P., Stevenson, D. S., Sudo, K., Szopa, S., and Zeng, G.: Radiative forcing since preindustrial times due to ozone change in the troposphere and the lower stratosphere, Atmos. Chem. Phys., 6, 575–599, doi:10.5194/acp-6-575-2006, 2006. 31608

ACPD
13, 31607–31634, 2013

SWIFT – a fast model for polar stratospheric ozone loss

M. Rex et al.

Hadjinicolaou, P., Pyle, J. A., and Harris, N. R. P.: The recent turnaround in stratospheric ozone over northern middle latitudes: a dynamical modeling perspective, Geophys. Res. Lett., 32, L12821, doi:10.1029/2005GL022476, 2005. 31609

Hanson, D. and Mauersberger, K.: Laboratory studies of the nitric acid trihydrate: Implications for the south polar stratosphere, Geophys. Res. Lett., 15, 855–858, 1988. 31620

Harris, N. R. P., Lehmann, R., Rex, M., and von der Gathen, P.: A closer look at Arctic ozone loss and polar stratospheric clouds, Atmos. Chem. Phys., 10, 8499–8510, doi:10.5194/acp-10-8499-2010, 2010. 31619

Hsu, J. and Prather, M. J.: Stratospheric variability and tropospheric ozone, J. Geophys. Res., 114, D06102, doi:10.1029/2008JD010942, 2009. 31609

Huck, P. E., Bodeker, G. E., Kremser, S., McDonald, A. J., Rex, M., and Struthers, H.: Semi-empirical models for chlorine activation and ozone depletion in the Antarctic stratosphere: proof of concept, Atmos. Chem. Phys., 13, 3237–3243, doi:10.5194/acp-13-3237-2013, 2013. 31610, 31621

Livesey, N. J., Read, W. G., Froidevaux, L., Lambert, A., Manney, G. L., Pumphrey, H. C., Santee, M. L., Schwartz, M. J., Wang, S., Cofeld, R. E., Cuddy, D. T.„ Fuller, R. A., Jarnot, R. F., Jiang, J. H., Knosp, B. W., Stek, P. C., Wagner, P. A., and Wu, D. L.: Version 3.3 Level 2 data quality and description document, JPL D-33509, available at: http://mls.jpl.nasa.gov, last access: November 2013, 2011. 31619

McLinden, C. A., Olsen, S. C., Hannegan, B. J., Wild, O., and Prather, M. J.: Stratospheric ozone in 3-D models: a simple chemistry and the cross-tropopause flux, J. Geophys. Res., 105, 14653–14665, 2000. 31609

Newman, P. A., Daniel, J. S., Waugh, D. W., and Nash, E. R.: A new formulation of equivalent effective stratospheric chlorine (EESC), Atmos. Chem. Phys., 7, 4537–4552, doi:10.5194/acp-7-4537-2007, 2007. 31619

Pitts, M. C., Thomason, L. W., Poole, L. R., and Winker, D. M.: Characterization of Polar Stratospheric Clouds with spaceborne lidar: CALIPSO and the 2006 Antarctic season, Atmos. Chem. Phys., 7, 5207–5228, doi:10.5194/acp-7-5207-2007, 2007. 31618

Rex, M., von der Gathen, P., Harris, N. R. P., Lucic, D., Knudsen, B. M., Braathen, G. O., Reid, S. J., De Backer, H., Claude, H., Fabian, R., Fast, H., Gil, M., Kyrö, E., Mikkelsen, I. S., Rummukainen, M., Smit, H. G., Stähelin, J., Varotsos, C., and Zaitcev, I.: In-situ measurements of stratospheric ozone depletion rates in the Arctic winter 1991/1992: a Lagrangian approach, J. Geophys. Res., 103, 5843–5853, 1998. 31619

ACPD
13, 31607–31634, 2013

SWIFT – a fast model for polar stratospheric ozone loss

M. Rex et al.

Rex, M., Salawitch, R. J., Deckelmann, H., von der Gathen, P., Harris, N. R. P., Chipperfield, M. P., Naujokat, B., Reimer, E., Allaart, M., Andersen, S. B., Bevilacqua, R., Braathen, G. O., Claude, H., Davies, J., De Backer, H., Dier, H., Dorokhov, V., Fast, H., Gerding, M., Godin-Beekmann, S., Hoppel, K., Johnson, B., Kyrö, E., Litynska, Z., Moore, D., Nakane, H., Parrondo, M. C., Risley Jr., A. D., Skrivankova, P., Stübi, R., Viatte, P., Yushkov, V., and Zerefos, C.: Arctic winter 2005: Implications for stratospheric ozone loss and climate change, Geophys. Res. Lett., 33, L23808, doi:10.1029/2006GL026731, 2006. 31622, 31634

Santee, M. L., MacKenzie, I. A., Manney, G. L., Chipperfield, M. P., Bernath, P. F., Walker, K. A., Boone, C. D., Froidevaux, L., Livesey, N. J., and Waters, J. W.: A study of stratospheric chlorine partitioning based on new satellite measurements and modeling, J. Geophys. Res., 113, D12307, doi:10.1029/2007JD009057, 2008. 31619

Solomon, S.: Stratospheric ozone depletion: a review of concepts and history, Rev. Geophys., 37, 275–316, 1999. 31612

von Hobe, M., Bekki, S., Borrmann, S., Cairo, F., D'Amato, F., Di Donfrancesco, G., Dörnbrack, A., Ebersoldt, A., Ebert, M., Emde, C., Engel, I., Ern, M., Frey, W., Genco, S., Griessbach, S., Grooß, J.-U., Gulde, T., Günther, G., Hösen, E., Hoffmann, L., Homonnai, V., Hoyle, C. R., Isaksen, I. S. A., Jackson, D. R., Jánosi, I. M., Jones, R. L., Kandler, K., Kalicinsky, C., Keil, A., Khaykin, S. M., Khosrawi, F., Kivi, R., Kuttippurath, J., Laube, J. C., Lefèvre, F., Lehmann, R., Ludmann, S., Luo, B. P., Marchand, M., Meyer, J., Mitev, V., Molleker, S., Müller, R., Oelhaf, H., Olschewski, F., Orsolini, Y., Peter, T., Pfeilsticker, K., Piesch, C., Pitts, M. C., Poole, L. R., Pope, F. D., Ravegnani, F., Rex, M., Riese, M., Röckmann, T., Rognerud, B., Roiger, A., Rolf, C., Santee, M. L., Scheibe, M., Schiller, C., Schlager, H., Siciliani de Cumis, M., Sitnikov, N., Søvde, O. A., Spang, R., Spelten, N., Stordal, F., Sumińska-Ebersoldt, O., Ulanovski, A., Ungermann, J., Viciani, S., Volk, C. M., vom Scheidt, M., von der Gathen, P., Walker, K., Wegner, T., Weigel, R., Weinbruch, S., Wetzel, G., Wienhold, F. G., Wohltmann, I., Woiwode, W., Young, I. A. K., Yushkov, V., Zobrist, B., and Stroh, F.: Reconciliation of essential process parameters for an enhanced predictability of Arctic stratospheric ozone loss and its climate interactions (RECONCILE): activities and results, Atmos. Chem. Phys., 13, 9233–9268, doi:10.5194/acp-13-9233-2013, 2013. 31612

WMO: World Meteorological Organization (WMO)/United Nations Environment Programme (UNEP), Scientific assessment of ozone depletion: 2010, Global Ozone Research and Monitoring Project – Report No. 52, 2011. 31621

Table 1. List of equations used in SWIFT.

Prognostic equations
$d[O_3]/dt = -D$
$d[ClONO_2]/dt = B - A - G - H$
$d[HCl]/dt = C + F - A$
$d[HNO_3]/dt = -E$
Diagnostic equations
$[ClO_x] = [Cl_y] - [HCl] - [ClONO_2]$
$[HNO_3]_g = [HNO_3] \cdot (1 - FAP) + z \cdot [HNO_3] \cdot FAP$

ACPD
13, 31607–31634, 2013

Table 2. List of the terms used in the differential equations.

Term	Expression	Remark
A	$a \cdot [ClONO_2] \cdot [HNO_3] \cdot FAP$ $a \cdot [HCl] \cdot [ClONO_2] \cdot [HNO_3] \cdot FAP$	for $[HCl] > 1\,\%$ of Cl_y for $[HCl] < 1\,\%$ of Cl_y
B	$b \cdot [HNO_3]_g \cdot FAS$ $b \cdot [ClO_x] \cdot [HNO_3]_g \cdot FAS$	for $[ClO_x] > 5\,\%$ of Cl_y for $[ClO_x] < 5\,\%$ of Cl_y
C	$c \cdot [ClO_x] \cdot FAS/[O_3]$	
D	$d \cdot [ClO_x] \cdot FAS$	
E	$e \cdot [HNO_3] \cdot \max((FAP - y), 0)$	
F	$f \cdot [ClO_x] \cdot FAS^2$ $0.25f \cdot [ClO_x] \cdot FAS^2$	Arctic Antarctic
G	$g \cdot [ClONO_2] \cdot FAS$	
H	$h \cdot [ClONO_2] \cdot \max((FAP - y), 0)$	

ACPD
13, 31607–31634, 2013

Table 3. List of parameters.

Parameter	Value
a	0.135292
b	0.437986
c	$1.578285 \cdot 10^{-3}$
d	$4.079051 \cdot 10^{-2}$
e	0.022993
f	0.209567
g	0.508703
h	0.455830
y	0.250000
z	0.579925

ACPD
13, 31607–31634, 2013

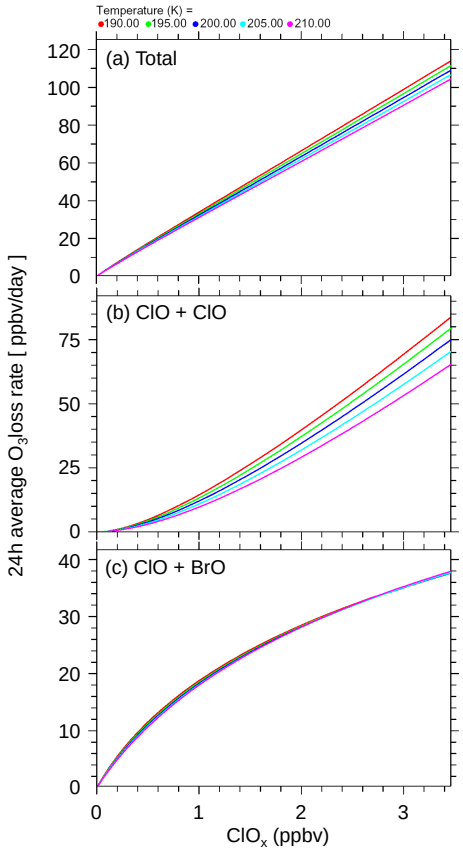

Fig. 1. 24 h ozone loss as a function of ClO_x mixing ratios. **(a)** Total, **(b)** by the ClO + ClO catalytic cycle, and **(c)** by the ClO + BrO catalytic cycle.

ACPD
13, 31607–31634, 2013

SWIFT – a fast model for polar stratospheric ozone loss

M. Rex et al.

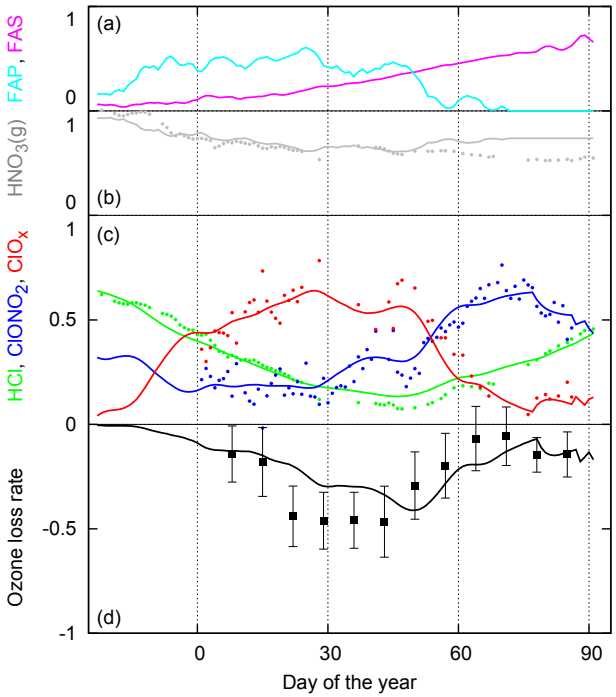

Fig. 2. Overview of SWIFT results and observations for the Arctic winter 2004/2005. All data are shown in normalized units (more details see text). **(a)** FAP (cyan) and FAS (magenta). Lines in **(b)–(d)** represent SWIFT results, dots represent vortex-averaged observations. **(b)** HNO_3 (gas phase, gray, observations from Aura MLS). **(c)** HCl (green, observations from Aura MLS), $ClONO_2$ (blue, observations from ACE-FTS), and ClO_x (red, "observed" ClO_x is derived by using a constant Cl_y minus the HCl and $ClONO_2$ observations). **(c)** Ozone loss rates (observations from Match). The loss rates of normalized ozone have been multiplied by 50 to facilitate plotting on the same scale. Error bars represent 1σ statistical uncertainties.

ACPD
13, 31607–31634, 2013

SWIFT – a fast model for polar stratospheric ozone loss

M. Rex et al.

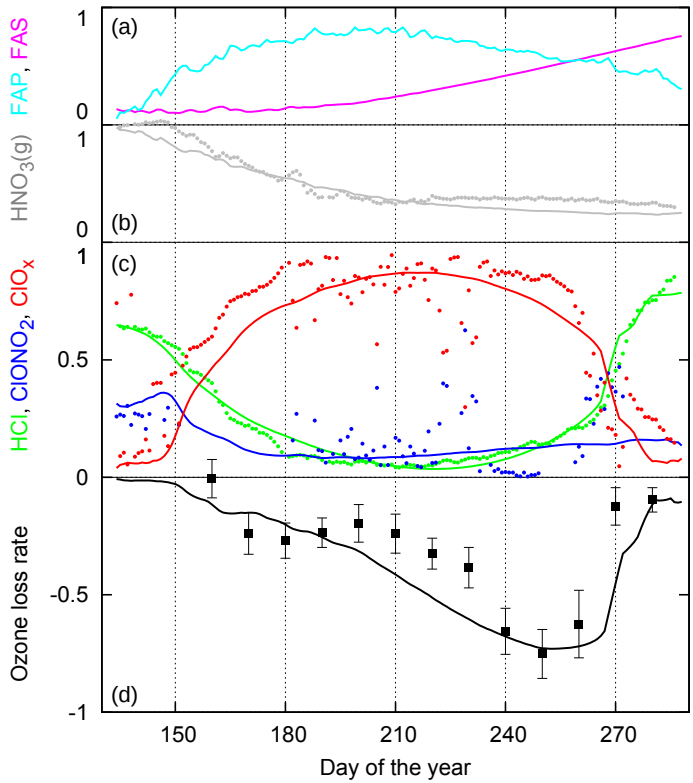

Fig. 3. As Fig. 2, but for the Antarctic winter 2006.

ACPD
13, 31607–31634, 2013

SWIFT – a fast model for polar stratospheric ozone loss

M. Rex et al.

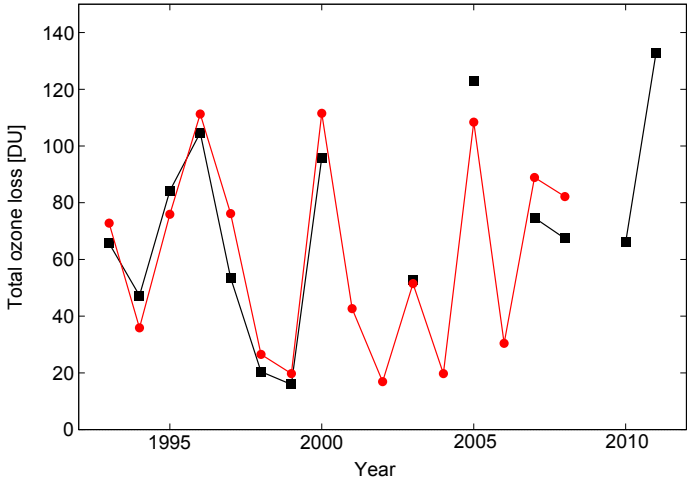

Fig. 4. Year-to-year variability in total chemical ozone loss in the Arctic estimated from SWIFT (red) compared with observations (black; Rex et al., 2006).

ACPD
13, 31607–31634, 2013